methods

High-throughput screening for fatty acid uptake inhibitors in humanized yeast identifies atypical antipsychotic drugs that cause dyslipidemias

Hong Li, Paul N. Black, Aalap Chokshi, Angel Sandoval-Alvarez, Ravi Vatsyayan, Whitney Sealls, and Concetta C. DiRusso[1]

Center for Metabolic Disease, Ordway Research Institute, Inc., and Center for Cardiovascular Sciences, Albany Medical College, Albany, NY 12208

Abstract **Fatty acids are implicated in the development of dyslipidemias, leading to type 2 diabetes and cardiovascular disease. We used a standardized small compound library to screen humanized yeast to identify compounds that inhibit fatty acid transport protein (FATP)-mediated fatty acid uptake into cells. This screening procedure used live yeast cells expressing human FATP2 to identify small compounds that reduced the import of a fluorescent fatty acid analog, 4,4-difluoro-5-methyl-4-bora-3a,4a-diaza-s-indacene-3-dodecanoic acid (C_1-BODIPY-C_{12}). The library used consisted of 2,080 compounds with known biological activities. Of these, ~1.8% reduced cell-associated C_1-BODIPY-C_{12} fluorescence and were selected as potential inhibitors of human FATP2-mediated fatty acid uptake. Based on secondary screens, 28 compounds were selected as potential fatty acid uptake inhibitors. Some compounds fell into four groups with similar structural features. The largest group was structurally related to a family of tricyclic, phenothiazine-derived drugs used to treat schizophrenia and related psychiatric disorders, which are also known to cause metabolic side effects, including hypertriglyceridemia. Potential hit compounds were studied for specificity of interaction with human FATP and efficacy in human Caco-2 cells. This study validates this screening system as useful to assess the impact of drugs in preclinical screening for fatty acid uptake.**—Li, H., P. N. Black, A. Chokshi, A. Sandoval-Alvarez, R. Vatsyayan, W. Sealls, and C. C. DiRusso. **High-throughput screening for fatty acid uptake inhibitors in humanized yeast identifies atypical antipsychotic drugs that cause dyslipidemias.** ***J. Lipid Res.*** **2008.** 49: **230–244.**

Supplementary key words fatty acid transport protein • 4,4-difluoro-5-methyl-4-bora-3a,4a-diaza-s-indacene-3-dodecanoic acid • yeast • Caco-2

During the past 20 years, obesity among adults and children has increased significantly in the United States. Being overweight or obese increases the risk for the development of adverse health conditions, including hypertension, dyslipidemia, diabetes, cardiovascular disease, and certain types of cancer, particularly colon and breast (1–6). It is hypothesized that high circulating levels of free fatty acids, occurring as a result of various metabolic disturbances, including overeating and diabetes, lead to excessive fatty acid internalization. Cell death results when the accumulation of these free fatty acids, especially saturated fatty acids, exceeds the cell's capacity for triglyceride storage, resulting in high levels of fatty acid oxidation, oxidative stress, and ceramide production (7, 8). This is termed lipotoxicity and is correlated with the development of obesity, insulin resistance, and cardiovascular disease (9–12). Therefore, it is desirable to target factors that contribute to fatty acid internalization and accumulation to prevent lipotoxicity.

Several lines of evidence favor the involvement of proteins in the import of exogenous fatty acids. First, fatty acid transport into cells is regulated by insulin, and emerging evidence shows that key transcriptional regulators, including peroxisome proliferator-activated receptor α, sterol-regulatory element binding protein 1, and retinoid X receptor, participate in these regulatory processes (13–16). Second, cells with high levels of fatty acid metabolism (either degradation or storage) transport fatty acids at higher rates compared with those with low levels of fatty acid metabolism (17, 18). Third, fatty acid transport is inducible in several different cell types and is commensurate with the expression of specific sets of proteins that are likely to participate in this process (19–21). Among these are the fatty acid transport proteins (FATPs) and long-

Manuscript received 14 June 2007 and in revised form 7 August 2007 and in re-revised form 13 September 2007 and in re-re-revised form 4 October 2007.

Published, JLR Papers in Press, October 10, 2007.
DOI 10.1194/jlr.D700015-JLR200

Abbreviations: ACSL, long-chain acyl-coenzyme A synthetase; AFU, arbitrary fluorescence unit; C_1-BODIPY-C_{12}, 4,4-difluoro-5-methyl-4-bora-3a,4a-diaza-s-indacene-3-dodecanoic acid; FAF BSA, fatty acid-free bovine-serum albumin; FATP, fatty acid transport protein; HTS, high-throughput screening; K_i, inhibition constant; MTT, 3-(4,5-dimethylthiazol-2-yl)-2,5-diphenyltetrazolium bromide; OD_{600}, optical density at 600 nm; YNBD, yeast minimal medium with dextrose; YPDA, yeast complete media with adenine.

[1] To whom correspondence should be addressed.
e-mail: cdirusso@ordwayresearch.org

chain acyl-coenzyme A synthetases (ACSLs) (22–24). The involvement of both FATP and ACSL is consistent with the model of vectorial acylation, in which fatty acid uptake is coupled to esterification with CoA (25–28). Our own work exploiting the genetically tractable yeast *Saccharomyces cerevisiae* has demonstrated that a membrane-bound FATP homolog, Fat1p, and an ACSL, either Faa1p or Faa4p, interact physically as well as functionally to catalyze import and activation (reviewed in Ref. 29). Fat1p and ACSL are both essential when cells are grown under hypoxic conditions, which render yeast auxotrophic for long-chain unsaturated fatty acids (30). Likewise, specific interactions have also been demonstrated between FATP1 and ACSL1 to potentiate fatty acid uptake in murine adipocytes (28). A number of studies have shown that fatty acid transport, particularly for protonated fatty acids, may also occur by diffusion or flip-flop between the two faces of the membrane (31–37). Using adipocytes, it was demonstrated that the association and flip-flop of oleate across the plasma membrane occurred very rapidly (33). A recent review of the diffusional model of fatty acid transport suggests that flip-flop is tied to the metabolic conversion to acyl-CoA, consistent with our model of vectorial acylation (32). Together, these reports provide compelling evidence for targeting fatty acid transport to limit the cellular uptake of fatty acids and thus lipotoxicity.

Previously, we developed a live cell high-throughput screening (HTS) assay using a *fat1Δfaa1Δ* yeast strain to identify chemical compounds that will inhibit fatty acid uptake (P. N. Black and C. C. DiRusso, United States Patent 7,070,944) (38). In this system, transport is a function of mouse FATP2 expressed from a yeast promoter and long-chain fatty acid activation is provided by the endogenous ACSL Faa4p. We demonstrated that this HTS assay is rapid to execute, inexpensive to implement, and has appropriate sensitivity for HTS. In the present work, we conducted a pilot study using a 2,080 compound library from MicroSource Discovery Systems, Inc. (Gaylordsville, CT), called SpectrumPlus® to improve and validate this live cell HTS method. We also devised secondary screens to eliminate false-positives in the yeast system and further evaluated the potential hit compounds using the human Caco-2 cell line. The members of the largest family of structurally related compounds identified in this screen are derivatives of a tricyclic phenothiazine core from which atypical antipsychotic drugs have been developed. Among these are chlorpromazine and the related compound clozapine. Many of the drugs in this class cause adverse side effects, including weight gain, hypertriglyceridemia, hyperglycemia, and ketoacidosis, which in severe cases have led to patient death (reviewed in Ref. 39). Consequently, several of these drugs have received black box warning labels. The mechanism by which these drugs cause these clinical symptoms is unknown. Our identification of these compounds as inhibitors of fatty acid uptake leads us to suggest that the metabolic dysregulation associated with the administration of these drugs is caused in whole or in part by reduced fatty acid uptake, resulting in the disruption of normal cellular lipid trafficking.

MATERIALS AND METHODS

Chemical compound library

The SpectrumPlus compound library (2,080 compounds) was obtained from MicroSource Discovery Systems, Inc. The library includes five subsets of compounds: *1*) Genesis Plus, composed of 960 compounds that represent new and classical therapeutic agents as well as established experimental inhibitors and receptor agonists; *2*) Pure Natural Products Collection, a unique collection of 720 diversified pure natural products and their derivatives, including simple and complex oxygen heterocycles, alkaloids, sequiterpenes, diterpenes, pentercyclic triterpenes, sterols, and many other diverse representatives; *3*) Agro Plate, containing 80 compounds representing classical and experimental pesticides, herbicides, and purported endocrine disruptors; *4*) Cancer Plate, including 80 cytotoxic agents, antiproliferative agents, immune suppressants, and other experimental and therapeutic agents; and *5*) Spectrum Plus Plate, containing 240 biologically active and structurally diverse compounds. The compounds are supplied as 10 mM solutions in DMSO and were diluted in PBS to a final concentration of 80 μM for screening in yeast using a Caliper RapidPlate 96/384 Dispenser (Caliper Life Sciences, Hopkinton, MA).

Reagents and cell culture

Yeast extract, yeast peptone, and yeast nitrogen base without amino acids and dextrose were obtained from Difco (Detroit, MI). Complete amino acid supplement and single amino acids were from Sigma (St. Louis, MO). Fatty acid-free bovine serum albumin (FAF BSA) and other chemical reagents were also from Sigma, unless stated otherwise. Corning® white with clear flat-bottom 96-well and 384-well microplates were used for screening of yeast. For Caco-2 cells, tissue culture-treated 96-well transparent with clear flat-bottom polystyrene microplates were from Fisher Scientific (Pittsburgh, PA). The fluorescent long-chain fatty acid analog, 4,4-difluoro-5-methyl-4-bora-3a,4a-diaza-s-indacene-3-dodecanoic acid (C_1-BODIPY-C_{12}), was obtained from the Molecular Probes Division of Invitrogen.

S. cerevisiae strain LS2086 containing deletions within the *FAT1* and *FAA1* genes (*fat1Δfaa1Δ; MATa ura3-52 his3Δ200 ade2-101 lys2-801 leu2-3,112 faa1::HIS3 fat1Δ::G418*) (26) was used for the primary screen. For most experiments, yeast minimal medium with dextrose (YNBD) contained 0.67% yeast nitrogen base (YNB), 2% dextrose, adenine (20 mg/l), uracil (20 mg/l), and amino acids as required [arginine, tryptophan, methionine, histidine, and tyrosine (20 mg/l); lysine (30 mg/l); and leucine (100 mg/l)]. When a rich medium was required (e.g., toxicity studies in yeast), yeast complete media with adenine (YPDA) was used. Growth in liquid culture and on plates was at 30°C.

Caco-2 cells were maintained in Earl's minimal essential medium with 20% FBS in a 95% air/5% CO_2 atmosphere at 37°C, as described previously (40). For growth and differentiation, the BD Biosciences Intestinal Epithelium Differentiation Media Pack was used. Cells were plated in basal seeding medium at a density of 2.5×10^5 cells/cm^2 on a collagen-coated black-clear 96-well plate (BD Biosciences). Entero-STIM medium was added to each well after removal of the basal seeding medium 24 h later. Both media contained mito-serum extender. After another 24 h, cells were washed once with complete balanced Hanks' solution containing Ca^{2+} and Mg^{2+} without phenol red before the C_1-BODIPY-C_{12} uptake assay.

Cloning and expression of human FATP2 in yeast

For expression of the human FATP2 in yeast, the cDNA encoding the protein was amplified using PCR from a cDNA within

NIH Image Clone I.D. 30348317 using forward primer 5′-gcatagccctcgagatgctttccgccatctacaca-3′ and reverse primer 5′-cgcagaccaagctttcagagtttcagggtttttagc-3′. The amplified DNA was cloned into the yeast expression vector pDB121 to give pDB126. In this construct, the expression of targeted human FATP2 is under the control of the *GAL10* promoter (41). The human FATP2 plasmid and pRS416GAL4-ER-VP16 encoding a synthetic transcriptional activator, which is a protein fusion between the Gal4 DNA binding domain, a β-estradiol-responsive regulatory domain, and a VP16 RNA polymerase activation domain (42), were cotransformed into strain LS2086 for HTS assays. Expression of human FATP was induced by the growth of yeast cells overnight in selective medium containing 10 nM β-estradiol. The level of human FATP2 protein was routinely measured using an antibody directed toward a T7 epitope fused to the C terminus of human FATP2 in Western blots of cell extracts.

HTS

For screening of the 2,080 compound MicroSource library, a Biomek® FX laboratory automated workstation (Beckman Coulter, Inc., Fullerton, CA) was used. LS2086 yeast cells expressing human FATP2 (pDB126/*fat1Δfaa1Δ*) or transformed with the empty vector pDB121 (negative control cells) were pregrown in YNBD without leucine and uracil (YNBD −leu −ura); the cells were subsequently subcultured to absorbance at 600 nm = 0.02 in the same medium containing 10 nM β-estradiol to induce expression and incubated overnight at 30°C with shaking. Mid-log-phase yeast cells [0.8–1.2 optical density at 600 nm (OD_{600})] were harvested and resuspended in PBS at a cell density of 6×10^7/ml before dispensing to a 384-well assay plate (22.5 μl/well). Wells in the first two rows of each plate received the negative control cells, and all other wells received cells expressing human FATP2. Compounds (2.5 μl) were then added to a final concentration of 80 μM. After 2 h of incubation at 30°C, the C_1-BODIPY-C_{12} uptake assay was performed. To each well, a mixture of C_1-BODIPY-C_{12} (final concentration, 1.25 μM), FAF BSA (final concentration, 0.75 μM), and trypan blue (final concentration, 2.1 mM) was added to give a final volume of 100 μl. Trypan blue quenched the extracellular fluorescence, and only cell-associated fluorescence was measured after 30 min on a Bio-Tek Synergy HT multidetection microplate reader (Bio-Tek Instruments, Inc., Winooski, VT) with filter sets of 485 ± 20 nm excitation and 528 ± 20 nm emission. On each plate, two rows each of negative control cells and positive control cells were incubated with 0.8% DMSO in PBS and assayed simultaneously to calculate a Z′ factor for each plate. The results presented are the values obtained for two screening experiments (see Tables 1, 3–7 below).

Determination of inhibition constant

Ligand competition curves were fit by nonlinear least-squares regression using a one-site competition model and Prism software (GraphPad Software, Inc., San Diego, CA) to determine the concentration of added competitor that reduced C_1-BODIPY-C_{12} fluorescence readout by 50% (IC_{50}). Inhibition constant (K_i) values were calculated from the IC_{50} by the equation of Cheng and Prusoff (43): $K_i = IC_{50}/(1 + [\text{radioligand}]/K_d)$, where radioligand is the concentration of C_1-BODIPY-C_{12} and K_d is the apparent affinity of C_1-BODIPY-C_{12} for the yeast cells expressing human FATP2 or Caco-2 cells. The apparent K_d was determined by measuring uptake activity in the presence of different C_1-BODIPY-C_{12} concentrations.

Toxicity assays

Wild-type yeast strain YB332 was used to evaluate the compound toxicity. Cells were grown in YPDA overnight and subcultured into the same medium at 0.1 OD_{600} in the presence of different concentrations of compound as indicated. Optical density was measured every hour during 8 h of growth. To test viability after treatment, cells were grown and treated with compound for 2 h as usual to test uptake inhibition but were harvested by centrifugation, washed three times with PBS, serially diluted, and plated on YPDA. After growth for 2 days at 30°C, colony numbers were counted and scored to give the number of colony-forming units per milliliter.

To evaluate potential toxic effects on Caco-2 cells, we used the MTT [for 3-(4,5-dimethylthiazol-2-yl)-2,5-diphenyltetrazolium bromide] assay (44). For these experiments, cells were treated with compound exactly as in the uptake assay using a 96-well format. At the end of the incubation period with test compound, the medium was removed and cells were treated with 100 μl of MEM containing 1.2 mM MTT for 3 h at 37°C. The reaction was terminated and cells were lysed by the addition of 5% SDS and 0.005 N HCl with incubation at 37°C for 1 h. The final absorbance was read at 570 nm to detect the formation of the purple formazan product. Cell viability was determined relative to a standard curve prepared using untreated cells.

Lipid analyses

To identify lipids labeled with C_1-BODIPY-C_{12}, LS2086 yeast cells (pDB126/*fat1Δfaa1Δ*) were grown in 50 ml of YNBD (−leu, −ura) containing 10 nM β-estradiol to 1.0 OD_{600} at 30°C. The culture was then concentrated by centrifugation and resuspended in PBS to a cell density of 6×10^7/ml. To half of the cell suspension, perphenazine (in PBS) was added to a final concentration of 40 μM; a control flask received PBS alone. Incubation with the compound continued for 2 h, then C_1-BODIPY-C_{12} (final concentration, 1.25 μM) in FAF BSA (final concentration, 0.75 μM) was added for 30 min to evaluate uptake. Metabolism was stopped by the addition of 0.1 volume of 6.6 M perchloric acid. Lipids were extracted essentially as detailed previously (45). After extraction, the dried lipids were resuspended in 50 μl of chloroform, and aliquots (5 μl) were spotted to Whatman Partisil LK5 TLC plates (250 μm, 150 Å silica). To resolve phospholipids, the solvent was a mixture of 25 ml of methyl acetate, 25 ml of 2-propanol, 28 ml of chloroform, and 7 ml of 0.25% KCl (solvent I); to resolve neutral lipids, the solvent consisted of three parts cyclohexane to two parts ethyl acetate (solvent II). All solvents were of HPLC grade and were obtained from Fisher Scientific. To detect C_1-BODIPY-C_{12}, the plates were scanned on a Bio-Rad Molecular Image FX scanner equipped with an external laser using filter sets of 488 nm excitation and 530 nm emission. Positions of the labeled lipids were compared with those of verified lipid standards (Sigma) resolved on the same TLC plates.

Visualization of C_1-BODIPY-C_{12} uptake into Caco-2 cells

Caco-2 cells were cultured as detailed above on four-well tissue culture-treated microscope slides (BD Falcon; BD Biosciences); two wells were used as controls and two wells were used for compound treatment. Treatment of cells with 80 μM perphenazine for 1 h and uptake of C_1-BODIPY-C_{12} were essentially as detailed for HTS with the following modifications. After treatment with compound or MEM (control), medium was removed and cells were washed with MEM. C_1-BODIPY-C_{12} (final concentration, 5 μM in 5 μM FAF BSA) was added for 3 min without trypan blue. Cells were then immediately rinsed with MEM, and Elvanol mounting medium was applied to each well. Cells were imaged using a Zeiss LSM510 confocal laser scanning microscope (Carl Zeiss MicroImaging, Inc., Thornwood, NY) equipped with a 63× objective using fluorescence modes. The instrument settings for

brightness and contrast were optimized to ensure that the confocal microscope was set for its full dynamic range relative to untreated cells on the same slide; the same settings were used for all subsequent image collections. An argon laser source was used for imaging, with excitation at 488 nm and emission at 505 nm.

Data analysis

Values in arbitrary units of the fluorescent signals from each HTS plate were exported to Excel (Microsoft Corp., Redmond, WA) spreadsheet templates, and the assay quality-control Z′ factor was calculated (46). ChemTree software (Golden Helix, Inc., Bozeman, MT) was used for additional statistical analysis and to study structure-activity relationships.

RESULTS

Library screening

In previous work, we developed a live cell, high-throughput method for the selection of small chemical modulators of fatty acid uptake dependent upon a murine FATP expressed in a *S. cerevisiae* strain deficient in the long-chain fatty acid transporter Fat1p and the major ACSL Faa1p (*fat1Δfaa1Δ*) (38). In this study, this strain was used to express the human FATP2 under the control of the *GAL10* promoter. Fatty acid uptake was measured as an increase in cell-associated fluorescence attributable to the accretion of the fluorescent fatty acid analog C_1-BODIPY-C_{12} through a human FATP2-dependent process. External fluorescence was quenched by the vital dye trypan blue. We used this system to screen a 2,080 chemical compound library, SpectrumPlus (MicroSource), to select for compounds that altered fatty acid uptake. This library consists of compounds that are structurally diverse, including known drugs, experimental actives, and pure natural products. The collection is advantageous in that the compounds included have been chosen for diversified structures containing unique structural scaffolds. Additionally, most compounds included in the set have known pharmacological and toxicological profiles that can be used to determine whether the hit compound or structur-

TABLE 1. Compounds that reduced cell-associated fluorescence in humanized yeast

Compound Identifier	Name	Percentage Transport Inhibition[a]	Comment
01500138	Benzethonium chloride	100, 100	
01500184	Chlorpromazine	100, 100	
01500315	Gentian violet	100, 100	Quenching agent
01503610	Benzalkonium chloride	100, 100	
01503253	Methylbenzethonium chloride	100, 100	
01503227	Perhexiline maleate	100, 100	
01503223	Pararosaniline pamoate	100, 100	Quenching agent
02300061	Clomipramine HCl	100, 100	
01500575	Thioridazine HCl	100, 100	
01505204	Almotriptan	100, 100	
00100325	Digitonin	100, 100	Membrane disruptor
01503934	Perphenazine	91, 100	
01503200	Centrimonium bromide	100, 96	
01504079	Tomatine	97, 98	Antimicrobial agent
01503936	Perciazine	72, 96	
01503637	Methiothepin maleate	59, 100	
01500127	Anthralin	81, 82	
00310035	Sanguinarine sulfate	53, 64	Antibiotic/antifungal agent
00201664	Celastrol	75, 97	Quenching agent
01503207	Cyclobenzaprine HCl	80, 86	
01505205	Olmesartan medoxomil	80, 98	
01502237	Harmol hydrochloride	89, 83	
01500473	Phenazopyridine hydrochloride	53, 51	
01500994	Flufenazine HCl	54, 99	
01504017	Sapindoside A	75, 92	Antifungal agent
01503239	Hycanthione	62, 69	
01500898	Emodin	74, 60	
01500685	Clozapine	66, 50	
00300038	Juglone	53, 47	Antifungal agent
01504119	Rhodomyrtoxin B	64, 40	
0300556	Chrysarobin	34, 42	
00211118	Diacetlydideisovaleryl-rhodomyrtoxin	45, 60	
01500759	Quinalizarin	70, 34	
01500602	Gossypol	40, 44	Quenching agent
01500510	Promethazine	44, 66	
01500509	Promazine	42, 46	
01500505	Prochlorperazine edisylate	45, 47	
00200022	Aklavin HCl	44, 69	
01504074	Embelin	44, 58	

[a] Percentage inhibition calculated from the ratio of fluorescence in arbitrary fluorescence units (AFU) for cells with compound compared with positive control cells with 0.8% DMSO alone. Results are from individual samples in two high-throughput screening trials (trial 1, trial 2).

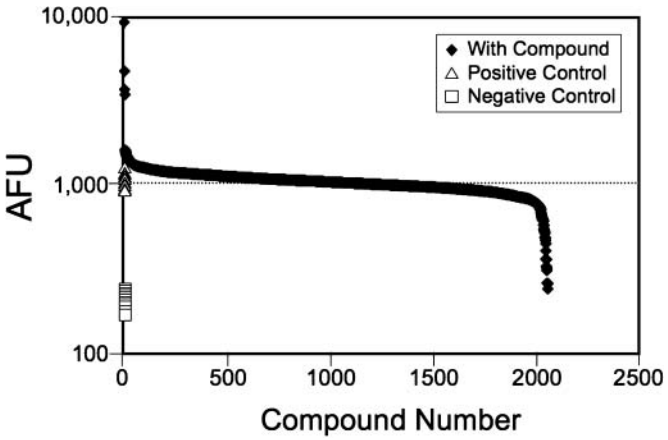

Fig. 1. High-throughput screening for fatty acid transport inhibitors. Cellular accumulation of 4,4-difluoro-5-methyl-4-bora-3a,4a-diaza-s-indacene-3-dodecanoic acid (C_1-BODIPY-C_{12}) was measured in arbitrary fluorescence units (AFU) for yeast cells expressing human fatty acid transport protein 2 (FATP2) after incubation with compounds (diamonds) or with DMSO (triangles; positive control). Accumulation of C_1-BODIPY-C_{12} in cells with empty vector was used as the negative control (squares). Compounds (80 μM in 0.8% DMSO) or DMSO alone were incubated with yeast cells expressing human FATP2 for 2 h at 30°C before C_1-BODIPY-C_{12} uptake assay. Data points are from one trial.

ally similar compounds can be safely and effectively prescribed for additional medicinal uses.

In our HTS, library compounds were tested at 80 μM on 384-well plates with yeast cells expressing the human FATP2. The fatty acid uptake activity of the cells was determined by comparing the cell-associated fluorescence of cells expressing human FATP2 with that of cells carrying the vector (pDB121) after incubation with the fatty acid analog C_1-BODIPY-C_{12} (38). The Z′ factors were calculated from values obtained from positive and negative controls (two lanes of each per plate) and ranged from 0.61 to 0.80, indicating a robust assay with good discrimination between the positive and negative controls (47). Two screening trials were performed, and there was excellent consistency between the two experiments. Potential inhibitors were identified using a cutoff value of 3 SD from the mean of the positive and negative controls (**Table 1**). As expected, most compounds (98%) had no effect on C_1-BODIPY-C_{12} uptake (**Fig. 1**). Four compounds enhanced the fluorescence signal, and 39 compounds were identified as potential inhibitors, as they reduced the cell-associated fluorescence compared with that of the cells incubated with vehicle alone. Of the 39 compounds, 22 (1.06%) reduced fluorescence by 80–100% and 17 (0.82%) gave intermediate levels (40–79% compared with positive controls).

Secondary screens eliminate autofluorescent and quenching compounds

This primary screening does not distinguish between effectors that alter apparent fluorescence readings by nonspecific mechanisms, apart from those that interact directly with FATP. Nonspecific effectors might include those that increase apparent fluorescence as a result of intrinsic properties specific to the compound or those compounds that act as quenching agents. Additionally, some compounds may disrupt membrane integrity and facilitate the internalization of trypan blue, which in turn quenches the imported fluorescent ligand. Therefore, all compounds identified as hits in the primary screen were subsequently tested for autofluoresence, the ability to quench C_1-BODIPY-C_{12} fluorescence, and the ability to disrupt membrane integrity (**Table 2**).

Two compounds identified in the primary screen, acriflavinium hydrochloride and calcein, yielded high intrinsic fluorescence that was not quenched by trypan blue, suggesting that these compounds did not enhance fatty acid uptake but increased fluorescence by nonspecific mechanisms (Fig. 1, Table 2). Sixteen of the 39 compounds that were hits from the primary screening were colored. These colored compounds might cause an inner filter effect, reducing the fluorescence signal of C_1-BODIPY-C_{12} as a result of overlap of their absorption spectrum with the emission spectrum of the BODIPY fluorophore. To test this concern, we determined the absorp-

TABLE 2. Tests to eliminate compounds with nonspecific effects, including autofluoresence, quenching, and membrane disruption

Compound Identifier	Compound Name	AFU Compound Alone[a]	AFU Compound with C_1-BODIPY-C_{12}[b]	AFU before Compound[c]	AFU after Compound[d]	Mechanism
01500618	Acriflavinium chloride	43,824	60,413	882	2,821	Autofluorescence
01503223	Pararosaniline pamoate	100	219	861	1,054	Quenching
00100325	Digitonin	108	28,371	802	420	Membrane disruption
01503934	Perphenazine	99	24,628	863	816	Unknown, potential hit
Positive controls[e]	NR	NR	NR	1,092	1,145	
Negative controls[f]	NR	NR	NR	240	286	

C_1-BODIPY-C_{12}, 4,4-difluoro-5-methyl-4-bora-3a,4a-diaza-s-indacene-3-dodecanoic acid; NR, not relevant.

[a] AFU of 80 μM compound with filter sets of 485 ± 20 nm excitation and 528 ± 20 nm emission as used to measure cell-associated C_1-BODIPY-C_{12}.

[b] Average AFU for 5 μM C_1-BODIPY-C_{12} alone was 24,361.

[c] Yeast cells expressing human fatty acid transport protein 2 were preloaded with 5 μM C_1-BODIPY-C_{12} under standard assay conditions and then fluorescence was measured.

[d] The same cell samples described in footnote *c* were incubated with 80 μM compound and incubated for 2 h at 30°C, then fluorescence was measured again.

[e] Yeast cells expressing human FATP2 as described in footnote *c* with 0.8% DMSO added and no compound.

[f] Yeast cells with vector incubated with 0.8% DMSO added and no compound.

tion spectrum of these compounds from 300 to 800 nm and found two structurally related compounds, gentian violet (purple) and pararosaniline pamoate (red), that have absorption maxima at 590 and 550 nm, respectively. Therefore, they most likely quench C_1-BODIPY-C_{12} fluorescence (emission at 510–625 nm). As expected, when these compounds were added directly to 5 μM C_1-BODIPY-C_{12} in the absence of cells, the fluorescence was reduced significantly (Table 2). These results showed that both compounds acted as quenching agents to cause the apparent reduction in cell-associated C_1-BODIPY-C_{12} fluorescence. Another compound, celastrol (orange), also modestly quenched the BODIPY fluorescence.

Compounds that act as membrane permeants will decrease cell-associated fluorescence because they will allow the vital dye trypan blue to enter the cells. Among these, the common detergent digitonin (48) is found in the SpectrumPlus library and was identified by its ability to reduce fluorescence to background levels. To eliminate compounds that disrupt membrane integrity, cells were preloaded with C_1-BODIPY-C_{12} in the presence of trypan blue for 30 min; each compound was added and cells were incubated for 2 h, then we revaluated cell-associated fluorescence. A reduction in fluorescence intensity after the addition of compound compared with fluorescence intensity before the addition of compound was interpreted as indicative of a loss of membrane integrity. Among the 39 compounds, only the cationic detergent digitonin acted as a strong membrane-permeabilizing agent using this test (Tables 1, 2). The SpectrumPlus library also contains at least one other cationic detergent, polymixin B sulfate. This compound weakly inhibited fatty acid uptake (~30% inhibition compared with positive controls) and was not included in the selected list of hits from our primary screen. Other compounds with known detergent-like properties, including centrimonium bromide (described below), did not affect fluorescence readings of cells preloaded with C_1-BODIPY-C_{12}.

Structural analysis of hit compounds in yeast

After eliminating the autofluorescent compounds and quenching and permeabilizing agents, we compared the structures of the remaining compounds to identify similar structural cores using ChemTree software. Using a multiple tree clustering algorithm, ChemTree automatically groups compounds that act according to similar quantitative structure-activity relationship mechanisms. Four groups of compounds that inhibited C_1-BODIPY-C_{12} uptake were thus identified as having similar structural scaffolds. Members of the first set are structurally related to the natural ligands of FATP, fatty acids, in that each has a long aliphatic hydrocarbon chain, including centrimonium bromide and benzalkonium chloride (**Table 3**). However, the hydrocarbon chain alone was not sufficient for the inhi-

TABLE 3. Compounds related to fatty acids with aliphatic, hydrocarbon chains

Compound Structure	Compound Name	Percentage Inhibition[a]
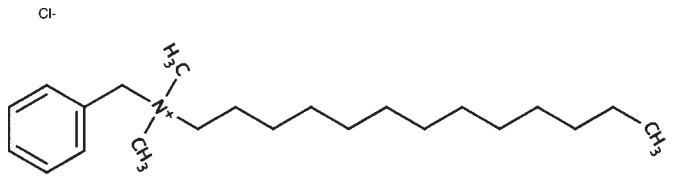	Benzalkonium chloride [ammonium, alkyldimethyl(phenylmethyl)-, chloride]	100, 100
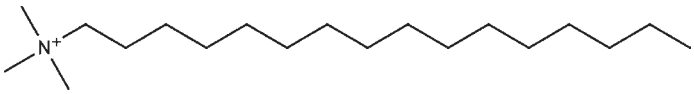	Centrimonium bromide (hexadecyl-trimethyl-ammonium, bromide)	100, 96
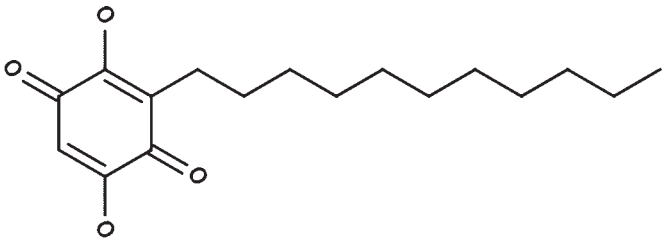	Embelin (2,5-dihydroxy-3-undecyl-cyclohexa-2,5-diene-1,4-dione)	44, 57
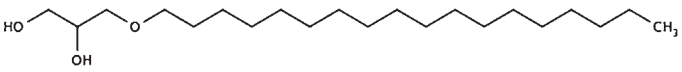	Batyl alcohol [3-(octadecyloxy)-1,2-propanediol]	0, 0
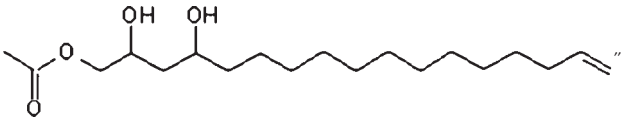	Avocadyne [(2,4-dihydroxyheptadec-16-ynyl) acetate]	0, 0

[a] Percentage inhibition compared with positive controls without compound. Results are for two experiments.

bition of C_1-BODIPY-C_{12} uptake, because at least five other compounds with this structural motif in the SpectrumPlus collection were inactive: batyl alcohol, roccellic acid, vocadyne acetate, avocadyne acetate, and caperatic acid. One compound, embelin, had intermediate activity. The inactive compounds have the common characteristic of being highly charged, with multiple hydroxyl groups on the terminal carbon of the chain that may preclude interaction with the transporter.

The largest number of hits that fell into one structural class was related to the phenazothiazines (**Table 4**). Five of these were highly active in preventing uptake,

TABLE 4. Compounds related to phenothiazine

Compound Structure	Compound Name	Percentage Inhibition[a]
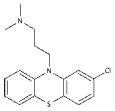	Chlorpromazine [3-(2-chlorophenothiazin-10-yl)-*N,N*-dimethyl-propan-1-amine]	100, 100
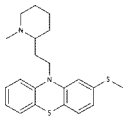	Thioridazine HCl [10-(2-(1-methyl-2-piperidyl)ethyl)-2-(methylthio)phenothiazine]	100, 100
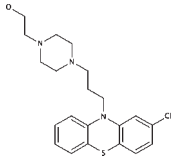	Perphenazine {2-[4-[3-(2-chlorophenothiazin-10-yl)propyl]piperazin-1-yl]ethanol}	91, 100
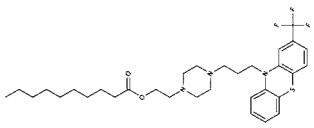	Flufenazine [2-(4-{3-[2-(trifluoromethyl)-10H-phenothiazin-10-yl] propyl}piperazin-1-yl)ethanol]	54, 99
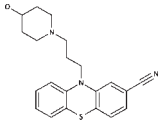	Periciazine {10-[3-(4-hydroxy-1-piperidyl)propyl] phenothiazine-2-carbonitrile}	72, 96
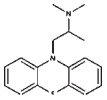	Promethazine (*N,N*-dimethyl-1-phenothiazin-10-yl-propan-2-amine)	45, 47
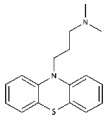	Promazine (*N,N*-dimethyl-3-phenothiazin-10-yl-propan-1-amine)	52, 46
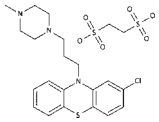	Prochlorperazine edisylate [2-chloro-10-(3-(1-methyl-4-piperazinyl)propyl)phenothiazine edisylate]	45, 47
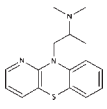	Isothiopendyl HCl [10H-pyrido(3,2-b) (1,4)benzothiazine, 10-(2-(dimethylamino)propyl)-]	0, 0
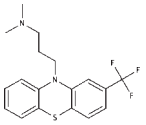	Triflupromazine {*N,N*-dimethyl-3-[2-(trifluoromethyl)phenothiazin-10-yl]propan-1-amine}	0, 0

[a] See Table 3 for details.

because cell-associated fluorescence remained at background levels. These included perphenazine, perciazine, chlorpromazine, thioridazine, and flufenazine. Three derivatives had intermediate activity (promethazine, promazine, and prochlorperazine edisylate) and two were completely inactive (isothiopendyl HCl and triflupromazine). To further assess the effects of this class of compounds on fatty acid uptake and metabolism, we compared C_1-BODIPY-C_{12} incorporation into lipids of yeast cells expressing human FATP2 treated either with PBS (control) or with perphenazine (**Fig. 2**). As expected, C_1-BODIPY-C_{12} was incorporated into both phospholipids and neutral lipids of control cells, and treatment with perphenazine substantially reduced the labeling of essentially all lipid classes.

A third group of related hit compounds contained a tricyclic core motif differing from the phenazothiazines in that the central ring has seven members rather than six (**Table 5**). The structures of these compounds are very similar, and subtle variations contribute to substantial differences in activity. Three compounds strongly inhibited uptake at 80 μM: clomipramine, methiothepin maleate, and cyclobenzaprine. Two were slightly active (clozapine and imipramine), whereas amitriptyline and loratadine were inactive.

The final set of compounds, although more structurally diverse within the group, were related in that all were heterocyclic and highly oxygenated (**Table 6**). These varied in the number of rings, from the simplest two-ring compound juglone to the five-ring structure of aklavin.

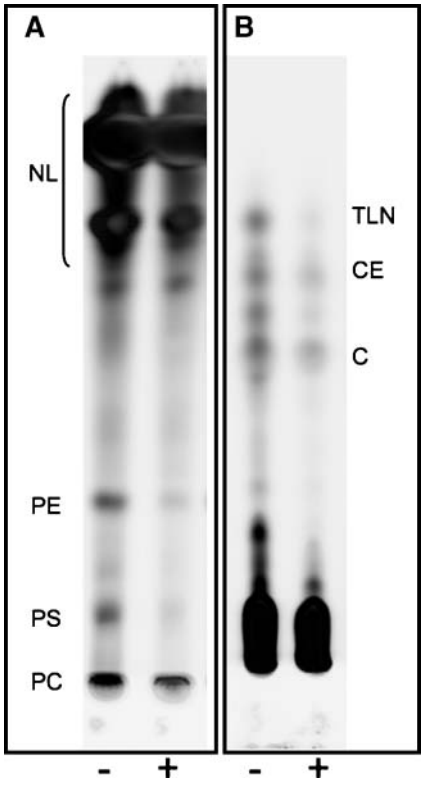

Fig. 2. Perphenazine inhibits the incorporation of the fluorescent fatty acid analog into various lipids. Lipids were isolated from yeast cells expressing human FATP2 after treatment with PBS (−) or perphenazine (+) and C_1-BODIPY-C_{12} as detailed in the text. A: Solvent system I was used to distinguish phospholipids from neutral lipids. B: Solvent system II was used to separate neutral lipids. Images shown are representative of two experiments. TLC plates were scanned using a phosphorimaging system. Positions of commercial standards are labeled as follows: NL, neutral lipids; PE, phosphatidylethanolamine; PS, phosphatidylserine; PC, phosphatidylcholine; TLN, triolean; CE, cholesteryl ester; C, cholesterol.

Toxic compounds are eliminated by evaluating yeast growth

We previously demonstrated that heat-killed cells become permeable to the fatty acid analog and the quenching agent trypan blue, resulting in low fluorescence readings using the C_1-BODIPY-C_{12} assay (38). This led us to question whether the mechanism of apparent inhibition of transport was merely attributable to cell death and associated membrane dysfunction. To test compound toxicity, wild-type yeast cells (YB332) were grown in YPDA to mid-log phase and then diluted to 0.1 OD_{600}. Serial dilutions of a test compound were added to medium, and growth of the yeast cells was monitored relative to cells incubated without the addition of compound. **Figure 3** shows the growth curves of YB332 in the presence of PBS (control) or 100 μM centrimonium bromide, anthralin, or perphenazine. At 100 μM, perphenazine seemed to inhibit the growth of yeast cells. Therefore, we further tested the viability of yeast cells in the presence of this putative inhibitory compound by plating cells on solid medium after treatment with compound for 2 h to mimic the conditions used in our HTS experiments. Using this method, >95% of the cells were viable. Therefore, we do not believe that inhibition by perphenazine was merely the result of cell death.

Evaluation of hit compounds in Caco-2 cells

Caco-2 cells are derived from a human colon adenocarcinoma (49). In culture, these cells spontaneously differentiate into polarized, columnar cells that are representative of the small intestine (50). When grown on plastic, they form domes typical of normal and transporting epithelium (51, 52). This cell line has been used extensively as a model for transport studies (50, 53). Previous work has shown that fatty acid uptake in Caco-2 cells is saturable, decreased by trypsin treatment of cells, and can be competed by natural fatty acids (54). These cells express higher levels of both FATP2 and FATP4 than other FATP isoforms (P. N. Black, P. Fraisl, and C. C. DiRusso, unpublished data). To further evaluate hit compounds identified from our screening of yeast cells, we performed C_1-BODIPY-C_{12} uptake inhibition experiments in 96-well format using Caco-2 cells. We initially tested the hit compounds in Caco-2 cells at 100 and 10 μM (**Table 7**). At 100 μM, most of these compounds inhibited Caco-2 uptake of C_1-BODIPY-C_{12} to varying extents. Seven compounds reduced uptake to essentially control levels, whereas most had intermediate activity. When the concentration of compound was de-

TABLE 5. Compounds related to cyclobenzaprine

Compound Structure	Compound Name	Percentage Inhibition[a]
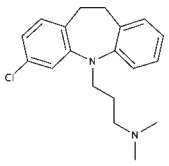	Clomipramine [3-chloro-5-(3-(dimethylamino)propyl)-10,11-dihydro-5H-dibenz(b,f)azepine]	100, 100
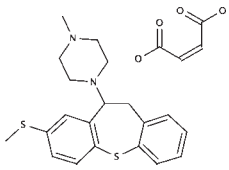	Methiothepin maleate [(+−)-1-(10,11-dihydro-8-(methylthio)dibenzo(b,f)thiepin-10-yl)-4-methylpiperazine]	59, 100
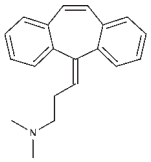	Cyclobenzaprine [1-propanamine, 3-(5H-dibenzo(a,d)cyclohepten-5-ylidene)-*N*,*N*-dimethyl- (9CI)]	80, 86
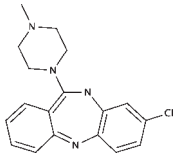	Clozapine [8-chloro-11-(4-methyl-1-piperazinyl)-5H-dibenzo(b,e) (1,4)diazepine]	66, 50
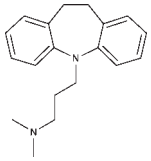	Imipramine [1-(3-dimethylaminopropyl)-4,5-dihydro-2,3,6,7-dibenzazepine]	0, 26
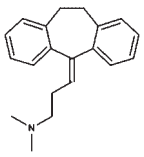	Amitriptyline HCl [10,11-dihydro-5-(γ-dimethylaminopropylidene)-5H-dibenzo(a,d)cycloheptene]	0, 0
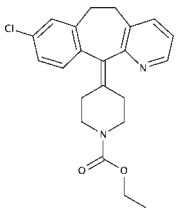	Loratadine [ethyl 4-(8-chloro-5,6-dihydro-11H-benzo(5,6)cyclohepta(1,2-b)pyridin-11-ylidene)-1-piperidinecarboxylate]	0, 0

[a] See Table 3 for details.

creased to 10 μM, only three compounds inhibited uptake by 25–40% of control levels (Table 7).

We next evaluated the concentration-dependent inhibition of centrimonium bromide, perphenazine, and anthralin on Caco-2 cells by comparison with yeast (**Fig. 4**). The results shown in Fig. 4B indicate that the K_i values of centrimonium bromide and perphenazine for Caco-2 cells was higher than that of yeast cells (Fig. 4A). For anthralin, we were unable to determine the K_i in Caco-2 cells, because at 200 μM the uptake was still ~70% of the control value. As was the case in yeast, C_1-BODIPY-C_{12} was incorporated into Caco-2 cells, labeled various cellular lipids, and did not show preferential compartmentalization (**Fig. 5**). Treatment with a representative compound, perphenazine, substantially reduced incorporation without causing cell death; at 80 μM perphenazine, there was 94 ± 9% cell survival, as estimated using the MTT cytotoxicity assay (five experiments).

TABLE 6. Compounds related to anthralin

Compound Structure	Compound Name	Percentage Inhibition[a]
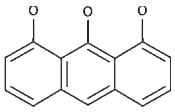	Anthralin (1,8,9-trihydroxyanthracene)	81, 82
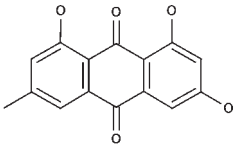	Emodin (1,3,8-trihydroxy-6-methyl-9,10-anthracenedione)	74, 60
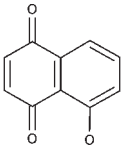	Juglone (5-hydroxy-1,4-naphthoquinone)	53, 47
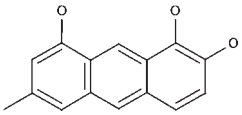	Chrysarobin (6-methylanthracene-1,2,8-triol)	34, 42
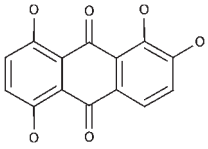	Quinazalin (1,2,5,8-tetrahydroxyanthracene-9,10-dione)	70, 34
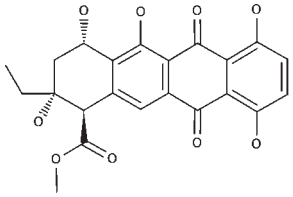	Rutilantinone [1-naphthacenecarboxylic acid, 1,2,3,4,6,11-hexahydro-2-ethyl-2,4,5,7,10-pentahydroxy-6,11-dioxo-, methyl ester, (1R,2R,4S)-]	3, 54
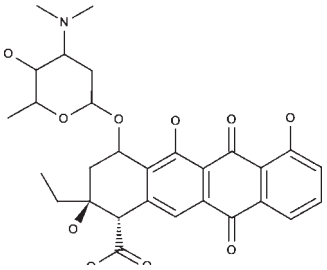	Aklavin [methyl (1S,2S)-4-(4-dimethylamino-5-hydroxy-6-methyl-oxan-2-yl)oxy-2-ethyl-2,5,7-trihydroxy-6,11-dioxo-3,4-dihydro-1H-tetracene-1-carboxylate hydrochloride]	44, 69
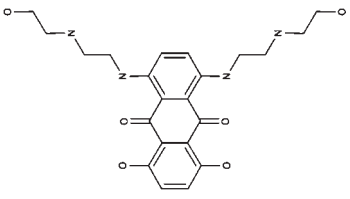	Mitoxanthrone [1,4-dihydroxy-5,8-bis(2-((2-hydroxyethyl)amino)ethylamino)-9,10-anthracenedione]	19, 39

[a] See Table 3 for details.

DISCUSSION

Validation of the screening method

In this study, we tested a HTS system for use in identifying fatty acid uptake inhibitors. The target of this HTS, the human fatty acid uptake system, is likely to be involved in the development and progression of many disease states that result from excessive intracellular accumulation of free fatty acids. We chose to use *S. cerevisiae* cells expressing the human FATPs for our primary screening because

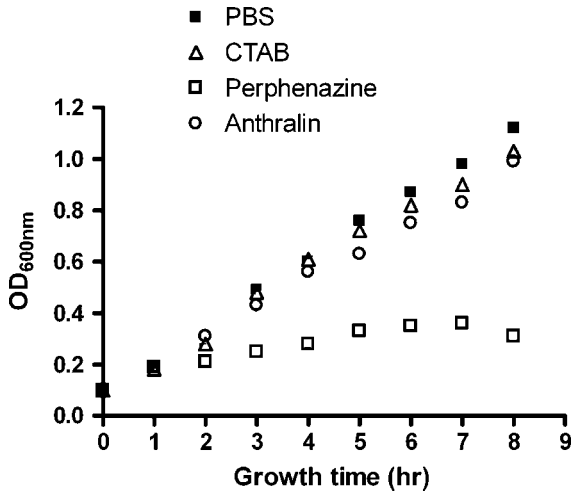

Fig. 3. Growth of yeast in the presence of selected hit compounds. Wild-type yeast was cultured in the presence of 100 μM compound as indicated; cells with an equivalent volume of 0.8% DMSO in PBS were included as a control. Growth was monitored at optical density at 600 nm over 8 h as shown. CTAB, centrimonium bromide.

1) the biochemistry and molecular genetics of fatty acid uptake in yeast are well understood and analogous to those of mammalian cell systems; *2*) phenotypic tests for fatty acid uptake and metabolism are readily available; *3*) yeast cells are small in size, grow rapidly, and are resistant to cell lysis upon automated manipulation; and *4*) the yeast HTS system is simple and inexpensive to implement. Our strategy was to carry out the HTS and initial screening for lead compounds using the humanized yeast system and then to analyze these compounds for their inhibition of fatty acid uptake in human cells. We validated this approach by screening a 2,080 compound library and identifying groups of compounds with similar chemical structures that inhibited fatty acid uptake in both yeast cells and human Caco-2 cells.

Hit compounds similar in structure to long-chain fatty acids

BODIPY-labeled fatty acids have been used to monitor fatty acid uptake (22, 26, 27) and have been shown to be biosynthetically incorporated into lipids of cells (55; this work) and cultured organs (56). The length of C_1-BODIPY-C_{12} is approximately equivalent to that of an 18-carbon fatty acid. Our laboratory also demonstrated that the uptake of this fluorescent fatty acid analog is effectively competed by the natural fatty acid oleate in yeast (38). In the present study, of 2,080 compounds screened, four groups of structurally related compounds were identified as hits as a result of inhibition of C_1-BODIPY-C_{12} uptake. Among these were two ionic detergents, centrimonium bro-

TABLE 7. Inhibition of fatty acid uptake in Caco-2 cells by compounds identified using humanized yeast

Identifier	Compound Name	Percentage Inhibition[a] (Experiment 1, Experiment 2) 100 μM	10 μM	Comment
01500138	Benzethonium chloride	91, 96	14, 14	
01500184	Chlorpromazine	43, 68	9, 9	
01500315	Gentian violet	95, 98	52, 53	Quenching agent
01503610	Benzalkonium chloride	88, 94	7, 8	
01503253	Methylbenzethonium chloride	90, 95	52, 53	
01503227	Perhexiline maleate	95, 98	9, 9	
01503223	Pararosaniline pamoate	57, 76	14, 14	Quenching agent
02300061	Clomipramine HCl	27, 58	5, 5	
01500575	Thioridazine HCl	42, 67	12, 12	
01505204	Almotriptan	10, 49	10, 10	
00100325	Digitonin	79, 97	18, 18	Membrane disruptor
01503934	Perphenazine	53, 74	14, 14	
01503200	Centrimonium bromide	39, 65	15, 15	
01504079	Tomatine	85, 92	9, 10	Antimicrobial agent
01503936	Perciazine	11, 49	9, 8	
01503637	Methiothepin maleate	11, 50	6, 5	
01500127	Anthralin	0, 42	15, 16	
00310035	Sanguinarine sulfate	30, 60	13, 13	
00201664	Celastrol	77, 88	19, 19	Quenching agent
01503207	Cyclobenzaprine HCl	2, 44	15, 15	
01505205	Olmesartan medoxomil	7, 47	18, 18	
01502237	Harmol hydrochloride	10, 48	6, 6	
01500473	Phenazopyridine hydrochloride	73, 87	40, 41	
01500994	Flufenazine HCl	41, 67	14, 15	
01504017	Sapindoside A	92, 63	0, 0	
01503239	Hycanthione	38, 65	16, 15	
01500898	Emodin	62, 79	31, 31	
00300038	Juglone	9, 48	0, 0	
01504119	Rhodomyrtoxin B	44, 68	15, 15	
0300556	Chrysarobin	17, 53	11, 11	
00211118	Diacetlydideisovaleryl-rhodomyrtoxin	46, 69	19, 19	
01500602	Gossypol	72, 80	23, 24	Quenching agent

[a] Percentage inhibition calculated from the ratio of fluorescence in AFU for cells with compound compared with positive control cells with DMSO alone. Results given are averages of triplicate samples for each of two experiments.

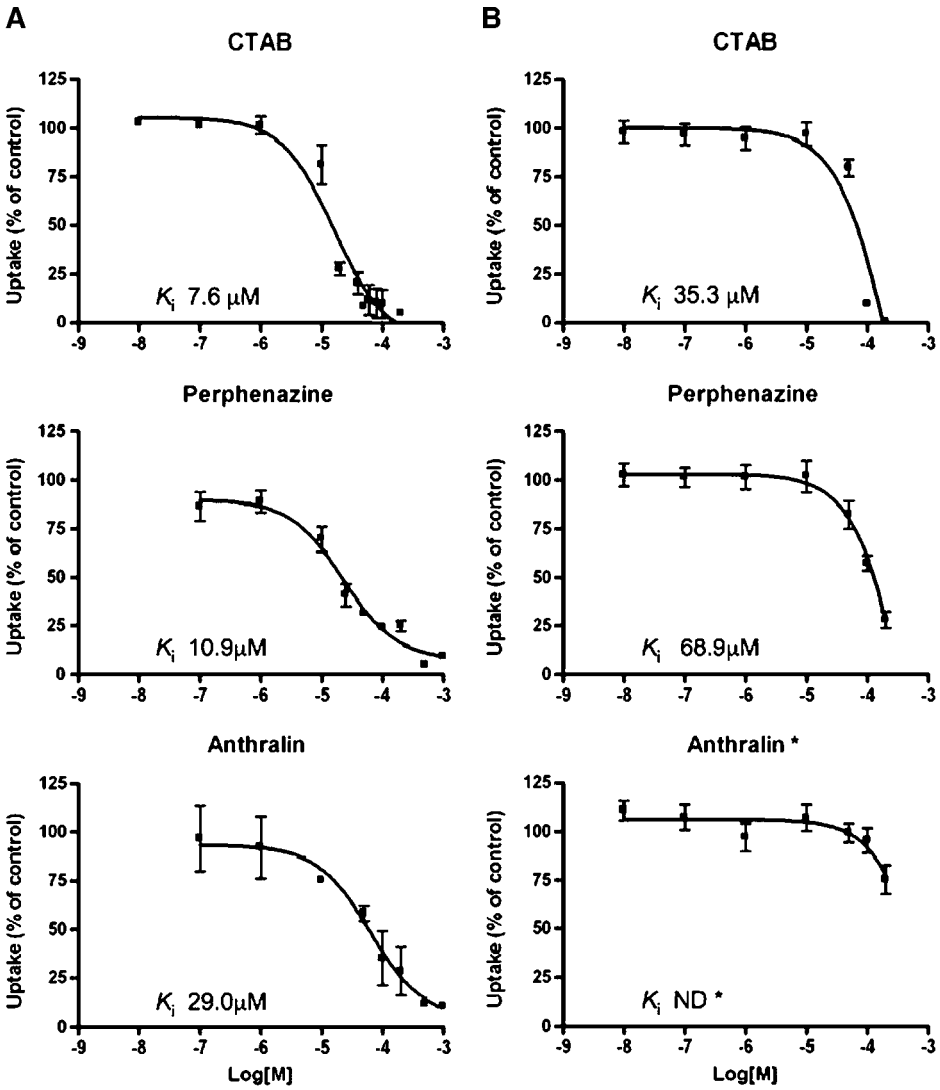

Fig. 4. Concentration dependence of the inhibition of uptake by centrimonium bromide (CTAB), perphenazine, and anthralin. The 100% of control values indicates values for cells incubated with PBS (yeast) or Hanks' balanced salt solution (Caco-2). A: Yeast cells expressing human FATP2 were incubated with compounds at 30°C for 2 h before uptake assay. B: Caco-2 cells were incubated with different concentrations of the compounds at 37°C for 1 h before uptake assay. * Anthralin at 200 μM kills Caco-2 cells. Data points are means of three experiments assayed in triplicate. Error bars indicate SEM. K_i, inhibition constant.

mide and benzalkonium chloride, which are similar to fatty acids in having a long hydrocarbon chain. These compounds may act as nonspecific detergents or may mimic fatty acids by interacting with FATP specifically, for example, by occupying the fatty acid binding site on the protein. We noted that these two compounds have critical micelle concentrations in the same range as cholic acid and deoxycholic acid (1–4 mM), which did not reduce apparent

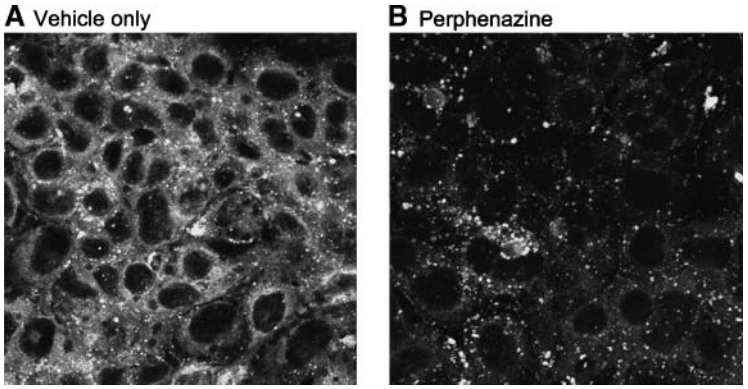

Fig. 5. Perphenazine blocks the incorporation of C_1-BODIPY-C_{12} into Caco-2 cells. Caco-2 cells were treated for 1 h with vehicle (MEM) alone (A) or 80 μM perphenazine followed by C_1-BODIPY-C_{12} for 3 min (B). Cells were imaged under fluorescence using confocal microscopy as detailed in the text.

fatty acid uptake, so nonspecific detergent effects do not adequately explain the inhibition of uptake by centrimonium bromide and benzalkonium chloride. Filipin, nystatin, and β-escin, three other compounds that disrupt cell wall and/or membrane architecture, also had no effect on uptake in our primary screening assay. Therefore, at the concentration used in these experiments (80 μM), it does not appear that these compounds disrupt FATP2-mediated fatty acid transport by nonspecific actions.

Some atypical antipsychotic drugs also inhibit uptake

The other two groups of compounds all have a three-ring structure similar to the BODIPY moiety of C_1-BODIPY-C_{12} (Tables 4, 5). One concern is that these compounds are merely competitive inhibitors of the fluorescent fatty acid analog and not the natural ligands. However, this is most likely not the case, because C_1-BODIPY-C_{12} is taken up in a FATP-specific manner and can be metabolized upon import. Furthermore, the native ligand (oleate) effectively competes with C_1-BODIPY-C_{12} (38). Thus, it is presumed the fluorescent ligand binds to the transporter in a manner analogous to the natural ligand. Compounds identified in this screen within these two structural classes fall into a family with well-known pharmacological properties that include antipsychotic drugs, which act by inhibition of neuroreceptors, including the dopamine receptor (39). Hints at a role for these compounds in fatty acid and lipid metabolism come from studies showing that these compounds are associated with hypertriglyceridemia, cholestatic liver, and insulin resistance (57, 58). A recent gene expression array study demonstrated a correlation between alterations in gene expression resulting from treatment of cells in culture with phenothiazine drugs and expression changes induced by treatment of cells with arachidonic acid (59). Together, these data strongly suggest that these drugs may affect lipid homeostasis in whole or in part through the inhibition of fatty acid uptake into cells. On the other hand, although these adverse side effects might seem to eliminate this class of compounds from consideration as potential fatty acid uptake inhibitors, they may prove useful in other ways. First, they will be valuable to understand the mechanisms causing the unwanted side effects of the drugs now in clinical use. Second, they potentially could be modified/rationally designed to interact more specifically with neuroreceptors rather than the FATP proteins and visa versa. Third, they are expected to be informative regarding mechanisms of FATP activity.

Few antifungal drugs in the library altered transport activity

Several compounds identified as hits were the antifungal agents tomatine, juglone, and sapinoside A. These compounds might act by killing the cell or inhibiting metabolic processes, including uptake. Because our primary screening assay requires only a 2 h incubation period with the compound, and because the addition of compound before C_1-BODIPY-C_{12} uptake did not result in reduced cell-associated fluorescence, we do not believe that these compounds are merely killing the cells. Cell death also results in increased membrane permeability. Metabolic poisoning might have the same effect in reducing membrane function, but this mechanism is more difficult to disprove with the types of assays available. We also note that the SpectrumPlus collection contains numerous antifungal agents that had no effect on C_1-BODIPY-C_{12} uptake by our method. Among these were fluconazole, griseofluvan, and clotrimazole.

In summary, we have designed multiple systems to identify and evaluate fatty acid uptake inhibitors. Primary screening and initial specificity evaluation used yeast cells that express a human FATP family member. Secondary screening has been developed in human cells (Caco-2) to verify and further evaluate the specificity of the lead compounds for inhibition of fatty acid uptake. This uptake assay has some aspects in common with another assay recently reported by Liao et al. (60). However, our method differs in that any cell type (from yeast to human cells) can be used with a high degree of sensitivity and reproducibility using an inexpensive quenching agent. In the future, we hope to use this method to identify compounds that discriminate between different classes of fatty acids or different FATP family members. Apart from identifying fatty acid uptake inhibitors, this system will also be of value in identifying fatty acid uptake activators. Additionally, although we have targeted human FATP-mediated fatty acid uptake in genetically defined yeast, modifications could be made in this system to target other participants in fatty acid transport, metabolism, and trafficking operative in living cells. Another anticipated use of this screening system is in determining whether or not lead drugs interfere with fatty acid uptake and metabolism before they enter whole animal or human trials. In this regard, this inexpensive, rapid, live cell assay should prove an adaptable secondary screen for this purpose.

Thanks are due to Mrs. Lori Bivins and Mrs. Jinhong Pan for technical assistance. This work was supported by grants from the Medical Technology Acceleration Program of the Charitable Leadership Foundation (Clifton Park, NY) and the National Institutes of Health (Grant DK-071076).

REFERENCES

1. Bray, G. A. 2003. Risks of obesity. *Endocrinol. Metab. Clin. North Am.* **32:** 787–804.
2. Cook, S., O. Hugli, M. Egli, P. Vollenweider, R. Burcelin, P. Nicod, B. Thorens, and U. Scherrer. 2003. Clustering of cardiovascular risk factors mimicking the human metabolic syndrome X in eNOS null mice. *Swiss Med. Wkly.* **133:** 360–363.
3. Lebovitz, H. E. 2003. The relationship of obesity to the metabolic syndrome. *Int. J. Clin. Pract. Suppl.* **134:** 18–27.
4. Semenkovich, C. F. 2004. Fatty acid metabolism and vascular disease. *Trends Cardiovasc. Med.* **14:** 72–76.
5. Westphal, S., G. H. Gekeler, J. Dierkes, H. Wieland, and C. Luley. 2002. A free fatty acid tolerance test identifies patients with coronary artery disease among individuals with a low conventional coronary risk profile. *Heart Vessels.* **16:** 79–85.

6. Wyne, K. L. 2003. Free fatty acids and type 2 diabetes mellitus. *Am. J. Med.* **115(Suppl. 8A):** 29–36.
7. Unger, R. H., and L. Orci. 2001. Diseases of liporegulation: new perspective on obesity and related disorders. *FASEB J.* **15:** 312–321.
8. Schrauwen, P., and M. K. Hesselink. 2004. Oxidative capacity, lipotoxicity, and mitochondrial damage in type 2 diabetes. *Diabetes.* **53:** 1412–1417.
9. Dubois, M., J. Kerr-Conte, V. Gmyr, T. Bouckenooghe, G. Muharram, M. D'Herbomez, A. Martin-Ponthieu, M. C. Vantyghem, B. Vandewalle, and F. Pattou. 2004. Non-esterified fatty acids are deleterious for human pancreatic islet function at physiological glucose concentration. *Diabetologia.* **47:** 463–469.
10. McGarry, J. D., and R. L. Dobbins. 1999. Fatty acids, lipotoxicity and insulin secretion. *Diabetologia.* **42:** 128–138.
11. Poitout, V., and R. P. Robertson. 2002. Minireview. Secondary beta-cell failure in type 2 diabetes—a convergence of glucotoxicity and lipotoxicity. *Endocrinology.* **143:** 339–342.
12. Robertson, R. P., J. Harmon, P. O. Tran, and V. Poitout. 2004. Beta-cell glucose toxicity, lipotoxicity, and chronic oxidative stress in type 2 diabetes. *Diabetes.* **53(Suppl. 1):** 119–124.
13. Berk, P. D., S. L. Zhou, C. L. Kiang, D. Stump, M. Bradbury, and L. M. Isola. 1997. Uptake of long chain free fatty acids is selectively up-regulated in adipocytes of Zucker rats with genetic obesity and non-insulin-dependent diabetes mellitus. *J. Biol. Chem.* **272:** 8830–8835.
14. Bonen, A., M. L. Parolin, G. R. Steinberg, J. Calles-Escandon, N. N. Tandon, J. F. Glatz, J. J. Luiken, G. J. Heigenhauser, and D. J. Dyck. 2004. Triacylglycerol accumulation in human obesity and type 2 diabetes is associated with increased rates of skeletal muscle fatty acid transport and increased sarcolemmal FAT/CD36. *FASEB J.* **18:** 1144–1146.
15. Coe, N. R., A. J. Smith, B. I. Frohnert, P. A. Watkins, and D. A. Bernlohr. 1999. The fatty acid transport protein (FATP1) is a very long chain acyl-CoA synthetase. *J. Biol. Chem.* **274:** 36300–36304.
16. Wu, Q., A. M. Ortegon, B. Tsang, H. Doege, K. R. Feingold, and A. Stahl. 2006. FATP1 is an insulin-sensitive fatty acid transporter involved in diet-induced obesity. *Mol. Cell. Biol.* **26:** 3455–3467.
17. Abumrad, N. A., C. C. Forest, D. M. Regen, and S. Sanders. 1991. Increase in membrane uptake of long-chain fatty acids early during preadipocyte differentiation. *Proc. Natl. Acad. Sci. USA.* **88:** 6008–6012.
18. Abumrad, N. A., J. H. Park, and C. R. Park. 1984. Permeation of long-chain fatty acid into adipocytes. Kinetics, specificity, and evidence for involvement of a membrane protein. *J. Biol. Chem.* **259:** 8945–8953.
19. Abumrad, N., C. Coburn, and A. Ibrahimi. 1999. Membrane proteins implicated in long-chain fatty acid uptake by mammalian cells: CD36, FATP and FABPm. *Biochim. Biophys. Acta.* **1441:** 4–13.
20. Memon, R. A., J. Fuller, A. H. Moser, P. J. Smith, C. Grunfeld, and K. R. Feingold. 1999. Regulation of putative fatty acid transporters and acyl-CoA synthetase in liver and adipose tissue in ob/ob mice. *Diabetes.* **48:** 121–127.
21. Frohnert, B. I., T. Y. Hui, and D. A. Bernlohr. 1999. Identification of a functional peroxisome proliferator-responsive element in the murine fatty acid transport protein gene. *J. Biol. Chem.* **274:** 3970–3977.
22. Schaffer, J. E., and H. F. Lodish. 1994. Expression cloning and characterization of a novel adipocyte long chain fatty acid transport protein. *Cell.* **79:** 427–436.
23. Glatz, J. F., J. J. Luiken, and A. Bonen. 2001. Involvement of membrane-associated proteins in the acute regulation of cellular fatty acid uptake. *J. Mol. Neurosci.* **16:** 123–132 (discussion 151–157).
24. Doege, H., and A. Stahl. 2006. Protein-mediated fatty acid uptake: novel insights from in vivo models. *Physiology (Bethesda).* **21:** 259–268.
25. Black, P. N., and C. C. DiRusso. 2003. Transmembrane movement of exogenous long-chain fatty acids: proteins, enzymes, and vectorial esterification. *Microbiol. Mol. Biol. Rev.* **67:** 454–472.
26. Zou, Z., F. Tong, N. J. Faergeman, C. Borsting, P. N. Black, and C. C. DiRusso. 2003. Vectorial acylation in *Saccharomyces cerevisiae.* Fat1p and fatty acyl-CoA synthetase are interacting components of a fatty acid import complex. *J. Biol. Chem.* **278:** 16414–16422.
27. DiRusso, C. C., H. Li, D. Darwis, P. A. Watkins, J. Berger, and P. N. Black. 2005. Comparative biochemical studies of the murine fatty acid transport proteins (FATP) expressed in yeast. *J. Biol. Chem.* **280:** 16829–16837.
28. Richards, M. R., J. D. Harp, D. S. Ory, and J. E. Schaffer. 2005. Fatty acid transport protein 1 and long chain acyl CoA synthetase 1 interact in adipocytes. *J. Lipid Res.* **47:** 665–672.
29. Black, P. N., and C. C. Dirusso. 2006. Yeast acyl-CoA synthetases at the crossroads of fatty acid metabolism and regulation. *Biochim. Biophys. Acta.* **1771:** 286–298.
30. Faergeman, N. J., C. C. DiRusso, A. Elberger, J. Knudsen, and P.N. Black. 1997. Disruption of the *Saccharomyces cerevisiae* homologue to the murine fatty acid transport protein impairs uptake and growth on long-chain fatty acids. *J. Biol. Chem.* **272:** 8531–8538.
31. Hamilton, J. A. 1999. Transport of fatty acids across membranes by the diffusion mechanism. *Prostaglandins Leukot. Essent. Fatty Acids.* **60:** 291–297.
32. Hamilton, J. A., and K. Brunaldi. 2007. A model for fatty acid transport into the brain. *J. Mol. Neurosci.* **33:** 12–17.
33. Kamp, F., W. Guo, R. Souto, P. F. Pilch, B. E. Corkey, and J. A. Hamilton. 2003. Rapid flip-flop of oleic acid across the plasma membrane of adipocytes. *J. Biol. Chem.* **278:** 7988–7995.
34. Kamp, F., and J. A. Hamilton. 1992. pH gradients across phospholipid membranes caused by fast flip-flop of un-ionized fatty acids. *Proc. Natl. Acad. Sci. USA.* **89:** 11367–11370.
35. Kamp, F., D. Zakim, F. Zhang, N. Noy, and J. A. Hamilton. 1995. Fatty acid flip-flop in phospholipid bilayers is extremely fast. *Biochemistry.* **34:** 11928–11937.
36. Zakim, D. 1996. Fatty acids enter cells by simple diffusion. *Proc. Soc. Exp. Biol. Med.* **212:** 5–14.
37. Pohl, E. E., U. Peterson, J. Sun, and P. Pohl. 2000. Changes of intrinsic membrane potentials induced by flip-flop of long-chain fatty acids. *Biochemistry.* **39:** 1834–1839.
38. Li, H., P. N. Black, and C. C. DiRusso. 2005. A live-cell high-throughput screening assay for identification of fatty acid uptake inhibitors. *Anal. Biochem.* **336:** 11–19.
39. Newcomer, J. W. 2005. Second-generation (atypical) antipsychotics and metabolic effects: a comprehensive literature review. *CNS Drugs.* **19(Suppl. 1):** 1–93.
40. Levy, E., M. Mehran, and E. Seidman. 1995. Caco-2 cells as a model for intestinal lipoprotein synthesis and secretion. *FASEB J.* **9:** 626–635.
41. DiRusso, C. C., E. J. Connell, N. J. Faergeman, J. Knudsen, J. K. Hansen, and P. N. Black. 2000. Murine FATP alleviates growth and biochemical deficiencies of yeast *fat1Δ* strains. *Eur. J. Biochem.* **267:** 4422–4433.
42. Stafford, G. A., and R. H. Morse. 1997. Chromatin remodeling by transcriptional activation domains in a yeast episome. *J. Biol. Chem.* **272:** 11526–11534.
43. Cheng, Y., and W. H. Prusoff. 1973. Relationship between the inhibition constant (K1) and the concentration of inhibitor which causes 50 per cent inhibition (I50) of an enzymatic reaction. *Biochem. Pharmacol.* **22:** 3099–3108.
44. Mosmann, T. 1983. Rapid colorimetric assay for cellular growth and survival: application to proliferation and cytotoxicity assays. *J. Immunol. Methods.* **65:** 55–63.
45. Faergeman, N. J., P. N. Black, X. D. Zhao, J. Knudsen, and C. C. DiRusso. 2001. The acyl-CoA synthetases encoded within *FAA1* and *FAA4* in *Saccharomyces cerevisiae* function as components of the fatty acid transport system linking import, activation, and intracellular utilization. *J. Biol. Chem.* **276:** 37051–37059.
46. Zhang, J. H., T. D. Chung, and K. R. Oldenburg. 1999. A simple statistical parameter for use in evaluation and validation of high throughput screening assays. *J. Biomol. Screen.* **4:** 67–73.
47. Zhang, J. H., T. D. Chung, and K. R. Oldenburg. 2000. Confirmation of primary active substances from high throughput screening of chemical and biological populations: a statistical approach and practical considerations. *J. Comb. Chem.* **2:** 258–265.
48. Karl, J., C. Gottfried, F. Tramontina, P. Dunkley, R. Rodnight, and C. A. Goncalves. 2000. GFAP phosphorylation studied in digitonin-permeabilized astrocytes: standardization of conditions. *Brain Res.* **853:** 32–40.
49. Fogh, J., J. M. Fogh, and T. Orfeo. 1977. One hundred and twenty-seven cultured human tumor cell lines producing tumors in nude mice. *J. Natl. Cancer Inst.* **59:** 221–226.
50. Hilgers, A. R., R. A. Conradi, and P. S. Burton. 1990. Caco-2 cell monolayers as a model for drug transport across the intestinal mucosa. *Pharm. Res.* **7:** 902–910.
51. Grasset, E., J. Bernabeu, and M. Pinto. 1985. Epithelial properties of human colonic carcinoma cell line Caco-2: effect of secretagogues. *Am. J. Physiol.* **248:** C410–C418.

52. Mohrmann, I., M. Mohrmann, J. Biber, and H. Murer. 1986. Sodium-dependent transport of Pi by an established intestinal epithelial cell line (CaCo-2). *Am. J. Physiol.* **250:** G323–G330.
53. Markowska, M., R. Oberle, S. Juzwin, C. P. Hsu, M. Gryszkiewicz, and A. J. Streeter. 2001. Optimizing Caco-2 cell monolayers to increase throughput in drug intestinal absorption analysis. *J. Pharmacol. Toxicol. Methods.* **46:** 51–55.
54. Ho, S. Y., and J. Storch. 2001. Common mechanisms of monoacylglycerol and fatty acid uptake by human intestinal Caco-2 cells. *Am. J. Physiol. Cell Physiol.* **281:** C1106–C1117.
55. Kasurinen, J. 1992. A novel fluorescent fatty acid, 5-methyl-BDY-3-dodecanoic acid, is a potential probe in lipid transport studies by incorporating selectively to lipid classes of BHK cells. *Biochem. Biophys. Res. Commun.* **187:** 1594–1601.
56. Sabah, J., E. McConkey, R. Welti, K. Albin, and L. J. Takemoto. 2005. Role of albumin as a fatty acid carrier for biosynthesis of lens lipids. *Exp. Eye Res.* **80:** 31–36.
57. Newcomer, J. W., and D. W. Haupt. 2006. The metabolic effects of antipsychotic medications. *Can. J. Psychiatry.* **51:** 480–491.
58. Kane, J. M., E. J. Barrett, D. E. Casey, C. U. Correll, A. J. Gelenberg, S. Klein, and J. W. Newcomer. 2004. Metabolic effects of treatment with atypical antipsychotics. *J. Clin. Psychiatry.* **65:** 1447–1455.
59. Lamb, J., E. D. Crawford, D. Peck, J. W. Modell, I. C. Blat, M. J. Wrobel, J. Lerner, J. P. Brunet, A. Subramanian, K. N. Ross, et al. 2006. The Connectivity Map: using gene-expression signatures to connect small molecules, genes, and disease. *Science.* **313:** 1929–1935.
60. Liao, J., R. Sportsman, J. Harris, and A. Stahl. 2005. Real-time quantification of fatty acid uptake using a novel fluorescence assay. *J. Lipid Res.* **46:** 597–602.